Parameter estimation of harmonics-polluted single-phase grid voltage signal

Pay, M. L. & Ahmed, H.

Parameter Estimation of Harmonics Polluted Single-Phase Grid Voltage Signal

Miao Lin Pay · Hafiz Ahmed

Abstract Estimation of instantaneous phase and frequency of harmonics polluted single-phase grid voltage signal have been studied in this paper. The proposed approach uses a frequency adaptive Luenberger Sliding Mode observer. Using Lyapunov stability theory, a frequency adaptation law has been proposed. The proposed frequency adaptive observer technique is robust against various perturbations faced in the practical settings e.g. discontinuous jump of phase, frequency and amplitude. Global stability analysis of the closed-loop observer has been performed. Experimental results demonstrate the effectiveness of the proposed technique over a state of the art technique proposed in the literature.

Keywords Power System · Phase Estimation · Frequency Estimation · PLL · Adaptive Observer

1 Introduction

Power electronics technology has enabled an increasing integration of renewable energy (solar, wind *etc.*) into the grid. In the context of grid integration of renewable energy sources, grid synchronization plays a huge role. Grid synchronization helps to connect an AC source (*e.g.* solar inverter) to the grid. Many types of grid synchronizing controllers requires the angular frequency or phase of the AC grid signal, *e.g.* proportional resonant (PR) controller (Fig. 1 in [34] *etc.*), reference frame transformation ($\alpha\beta \rightarrow dq$) inside the inner current control loop (*cf.* Fig. 1 in [36]). An accurate grid synchronization helps to reduce the total harmonic distortion (THD). Moreover, it ensures the in-phase relationship between the grid voltage and currents resulting in the enhancement of stability of grid-connected inverter systems .

M.L. Pay
Department of Engineering and Technology, University of Hertfordshire, College Lane, Hatfield, AL10 9AB, United Kingdom
E-mail: mp19abs@herts.ac.uk
H. Ahmed
School of Mechanical, Aerospace and Automotive Engineering, Coventry University, Priory Street, CV1 5FB, United Kingdom.
E-mail: hafiz.h.ahmed@ieee.org

Due to the important role of grid synchronization, many techniques have been developed and proposed in the literature. discrete Fourier transform (DFT) [20], fuzzy logic [24], statistical techniques [14,25], self-tuning filter [10,12,11], regression techniques: least-squares (linear and nonlinear, recursive, weighted *etc.*) [35], the Kalman filter (linear, extended, unscented *etc.*) [19], phase-locked loop (PLL) [21,23,33,9,22], frequency-locked loop (FLL) [29,6,1,26,7], adaptive notch filter (ANF) [13], neural networks [27] *etc.* are some of the most commonly used techniques.

Frequency domain techniques like DFT [20] are appropriate for harmonic detection applications. However the presence of harmonics increase the computational burden enormously as large window size is required. Moreover, numerous parameters need to be tuned. Least-square and Kalman filters [35,19] based techniques require less parameters to tune. However, they use online matrix inverse. Online matrix inverse is computationally demanding and limits the switching frequency in micro-controller based applications. Lower switching frequency implies bigger and heavier filter inductor. Moreover, Kalman filters use coordinate transformation which increases computational burden further. To overcome the high computational burden, adaptive notch filter (ANF) [13] can be a good alternative. However, in the presence of harmonics, steady-state error is inevitable.

Out of various techniques, PLL [21,23,33,9,22,4] received wide spread attention due to its excellent performances yet having a simple structure. However, in the case of simple PLL, there is a trade-off between accuracy and fast dynamic response. To overcome this trade-off, numerous modifications are proposed. Modified or Enhanced PLLs generally have good dynamic performance with respect to traditional PLLs but comes at a cost of higher computational resources. Moreover, small oscillations may also be observed in the presence of non-ideal frequency. Second order generalized integrator - frequency-locked loop (SOGI-FLL) [29,3] and its various variants are another popular technique used widely in the literature. However, SOGI-FLL uses linear harmonic oscillator structure. As reported in the literature [17], linear harmonic oscillators are not structurally stable. Infinitesimally small perturbations may change the type of the equilibrium point to a stable focus (decaying oscillation) or unstable focus (growing oscillation). Moreover, the amplitude of oscillation depends on the initial conditions. From the literature review, it is clear that there are scopes to improve the existing results.

One of the major power quality issue in grid synchronizing control design is the presence of harmonics in the grid voltage waveform. When harmonics are present, steady-state error becomes a major issue. In this work, the authors focus on the estimation of phase and frequency of single-phase grid voltage signal in the presence of harmonics. To get zero steady-state error in the presence of harmonics, researchers came up with different ideas. One way is to use filtering to eliminate the harmonic components of the grid signal. However, filtering introduces delay. Moreover, filtered signal can't be used for amplitude estimation. Another approach is to use higher order methods *e.g.* multiple PLL tuned at different harmonic frequencies. Higher order approaches can eliminate the steady-state error completely. Moreover, tuning is simpler as the fundamental building block is the same. Example of higher order approach can be found in [29]. Similar approach is considered in this work.

In this work, we propose a time-domain technique for the estimation of the phase and frequency of single-phase grid voltage signal. In comparison to the other time-domain techniques, our method is free from PLL, no complex filtering or quadrature signal generator (QSG) is required. Instead, we consider the grid-voltage as a time-

varying dynamical systems. Then we design a frequency adaptive Luenberger Sliding Mode (LSM) observer for this dynamical system. The proposed LSM observer is inspired by the ideas presented in [16, 2, 18, 32, 8, 5]. In the article, we have extended the work of [2] for the case of harmonics. Moreover, a novel parameter identification law is also introduced. Our approach is easy to use and implement. Finally, using Lyapunov function based approach, global stability analysis is also provided.

The rest of the article is organized as follows: details of the proposed observer based estimation is given in Sec. 2. Real-time controller platform dSPACE based experimental results are given in Sec. 3. Finally Sec. 4 concludes this article.

2 Parameter Estimation Approach

Harmonics polluted single-phase grid-voltage signal can be written as:

$$y = \nu_1 \sin \underbrace{(2\pi f_1 t + \varphi_1)}_{\theta_1} + \nu_2 \sin \underbrace{(2\pi f_2 t + \varphi_2)}_{\theta_2} + \cdots$$

$$+ \nu_n \sin \underbrace{(2\pi f_n t + \varphi_n)}_{\theta_n}$$

$$= \sum_{i=1}^{n} \nu_i \sin \underbrace{(2\pi f_i t + \varphi_i)}_{\theta_i}, i = 1, 2, \ldots, n \tag{1}$$

where $x_i, i = 1, 2, \ldots, n$ is the individual harmonic voltage signal, $\nu_i, f_i, \varphi_i, i = 1, 2, \ldots, n$ are the amplitude, frequency and phase of the individual frequency components and $\theta_i \in [0, 2\pi), i = 1, 2, \ldots, n$ represents the phase angle of the each frequency components. In this work, we assume that f_i in eq. (1) is unknown but constant. In practice, f_i may not be constant and subject to disturbance like step change of frequency. However, through experimental results in Sec. 3, we demonstrate that our proposed technique can successfully track time varying frequency. The constant frequency assumption is only for mathematical convenience.

Let us consider that

$$\dot{x}_j = x_{j+1} = \nu_i 2\pi f_i \cos \left(2\pi f_i t + \varphi_i \right), i = 1, 2, \ldots, n, j = 1, 3, \ldots, 2n - 1$$

Moreover, individual frequency f_i is related to the fundamental component through the following relationship

$$f_i = j f_1, i = 1, 2, \ldots, n, j = 1, 3, \ldots, 2n - 1$$

The fundamental component i.e. f_1 is related to the nominal known frequency through the following relationship:

$$\kappa = f_1^2/f_n^2 \tag{2}$$

where f_n is the known nominal grid frequency *i.e.* 60Hz in the USA and 50Hz in Europe. If the actual grid frequency is the same as the nominal frequency, then $\kappa = 1$. Then, in the state-space framework, the dynamics of the individual harmonic grid voltage signal, x_j and its derivative $\dot{x}_j = x_{j+1}$, can be written as:

$$\dot{x} = \bar{A}x,$$
$$y = \bar{C}x \tag{3}$$

where

$$x = \begin{bmatrix} x_1 \\ x_2 \\ x_3 \\ x_4 \\ \vdots \\ x_{2n-1} \\ x_{2n} \end{bmatrix} = \begin{bmatrix} \nu_1 \sin(2\pi f_1 t + \varphi_1) \\ \nu_1 2\pi f_1 \cos(2\pi f_1 t + \varphi_1) \\ \nu_2 \sin(2\pi f_2 t + \varphi_2) \\ \nu_2 2\pi f_2 \cos(2\pi f_2 t + \varphi_2) \\ \vdots \\ \nu_n \sin(2\pi f_n t + \varphi_n) \\ \nu_n 2\pi f_n \cos(2\pi f_n t + \varphi_1) \end{bmatrix},$$

$$\bar{A} = \begin{bmatrix} 0 & 1 & 0 & 0 & \cdots & 0 & 0 \\ -\omega_1^2 & 0 & 0 & 0 & \cdots & 0 & 0 \\ 0 & 0 & 0 & 1 & 0 & 0 & 0 \\ 0 & 0 & -\omega_2^2 & 0 & 0 & \vdots & \vdots \\ 0 & 0 & 0 & 0 & \ddots & 0 & 0 \\ \vdots & \vdots & \vdots & \vdots & 0 & 0 & 1 \\ 0 & 0 & 0 & 0 & 0 & -\omega_n^2 & 0 \end{bmatrix},$$

$$\bar{C} = \begin{bmatrix} 1 & 0 & 1 & 0 & \dots & 1 & 0 \end{bmatrix}$$

where $\omega_i^2 = (2\pi f_i)^2 = \kappa\{jf_n\}^2$ for $i = 1, 2, \dots, n, j = 1, 3, \dots, 2n - 1$. Using Kalman rank condition, it can be seen that the system (3) is observable as

$$\text{rank}([C\ CA\ \dots\ CA^{n-1}]) = \text{rank}(A) = n$$

.

For system (3), estimating the parameters ν_i, f_i and θ_i is essentially the problem of state observation. Matrix $\bar{A}$ and $\bar{C}$ are very useful for observer design. However, from numerical point of view, it is often difficult to construct an observer with matrices $\bar{A}$ and $\bar{C}$. As such coordinate transformations are often used (see [30]).

Let us consider the following coordinate transformation

$$z = Tx \tag{4}$$

where

$$T = \begin{bmatrix} T_1 & 0 & \cdots & 0 \\ 0 & T_2 & \vdots & \vdots \\ \vdots & 0 & \ddots & 0 \\ 0 & \cdots & 0 & T_n \end{bmatrix},$$

$$T_i = \begin{bmatrix} \frac{(2\pi f_i)^{-2}}{\kappa+1} & -\frac{(2\pi f_i)^{-3}}{\kappa+1} \\ \frac{\kappa(2\pi f_i)^{-1}}{\kappa+1} & \frac{(2\pi f_i)^{-2}}{\kappa+1} \end{bmatrix}$$

Dynamics of the system (3) in the new coordinate (4), can be written as:

$$\begin{aligned} \dot{z} &= T\dot{x} \\ &= T\bar{A}x \\ &= T\bar{A}T^{-1}z \\ \dot{z} &= Az \\ y &= Cz \end{aligned} \tag{5}$$

where $A = T\bar{A}T^{-1} = \bar{A}$ and

$$C = \bar{C}T^{-1} = [(2\pi f_n)^2 \quad 2\pi f_n \quad (6\pi f_n)^2 \quad (6\pi f_n)...$$
$$(2\pi j f_n)^2 \quad 2\pi j f_n].$$

For the transformed system (5), motivated by the ideas presented in [16], the following Luenberger-sliding mode observer is proposed:

$$\begin{aligned} \eta &= \hat{A}\eta + L(y - C\eta) + K\mathrm{sgn}(y - C\eta) \\ \hat{y} &= C\eta \end{aligned} \tag{6}$$

where η is the estimate of z, L is the gain matrix of the Luenberger part of the observer satisfying $\mathcal{R}\{\lambda(A - LC)\}|_{\kappa=1} < 0$, K is gain matrix of the sliding mode part of the observer, $\hat{\kappa}$ is the estimate of κ,

$$\hat{A} = \begin{bmatrix} \hat{A}_1 & 0 & \cdots & 0 \\ 0 & \hat{A}_2 & \vdots & \vdots \\ \vdots & 0 & \ddots & 0 \\ 0 & \cdots & 0 & \hat{A}_n \end{bmatrix},$$

$$\hat{A}_i = \begin{bmatrix} 0 & 1 \\ -\hat{\kappa}(2\pi j f_n)^2 & 0 \end{bmatrix}$$

and the sign function is defined as:

$$\mathrm{sgn}(x) := \begin{cases} -1 & x < 0 \\ 0 & x = 0 \\ 1 & x > 0 \end{cases}.$$

Observer (6) is discontinuous. As such the solution of (6) is to be understood in the sense of Filippov [15].

2.1 Stability analysis of the observer

To check the convergence or stability of the observer (6), let us consider the following output estimation error:

$$\delta = Cz - C\eta$$
$$\dot{\delta} = C\dot{z} - C\dot{\eta}$$
$$= CAz - C\hat{A}\dot{\eta}$$
$$= CAz - C\{\hat{A}\eta + L(y - C\eta) + K\mathrm{sgn}(y - C\eta)\}$$
$$\dot{\delta} = C(A - LC)(z - \eta) - C\left(\hat{A} - A\right)\eta - CK\mathrm{sgn}(\delta) \tag{7}$$

With the state estimation error dynamics (7), let us consider the following Lyapunov function candidate [16]:

$$V(\delta, \kappa - \hat{\kappa}) = \delta^T \delta + (\kappa - \hat{\kappa})^2 \tag{8}$$

Lyapunov function $V(\delta, \kappa - \hat{\kappa}) = 0$ for $\delta, \kappa - \hat{\kappa} = 0$ and positive otherwise. Evaluating the total derivative of V, along the solutions of (7), we obtain

$$\dot{V}(\delta, \kappa - \hat{\kappa}) = \delta^T\dot{\delta} + \dot{\delta}^T\delta - 2(\kappa - \hat{\kappa})\dot{\hat{\delta}}$$

$$\dot{V}(\delta, \kappa - \hat{\kappa}) = \underbrace{2(z - \eta)^T C^T C(A - LC)(z - \eta) - 2\delta^T CK\mathrm{sign}(\delta)}_{\#1}$$
$$\underbrace{-2(\kappa - \hat{\kappa})\dot{\hat{\delta}} - 2\eta^T(\hat{A} - A)^T C^T \delta}_{\#2} \tag{9}$$

The term #1 in eq. (9) is always less than or equal to zero for properly tuned matrix L and K (see Sec. 2.2 for details). Next,

$$\eta^T\left(\hat{A} - A\right)^T C^T \delta$$

$$= \begin{bmatrix} \begin{pmatrix} \eta_1 \\ \eta_2 \\ \vdots \\ \eta_{2n-1} \\ \eta_{2n} \end{pmatrix} \end{bmatrix}^T \left(\begin{bmatrix} \beta_1 & 0 & \cdots & 0 \\ 0 & \ddots & 0 & \vdots \\ \vdots & & \ddots & 0 \\ 0 & \cdots & 0 & \beta_n \end{bmatrix} \begin{pmatrix} \begin{pmatrix} (2\pi f_n)^2 \\ 2\pi f_n \end{pmatrix} \\ \begin{pmatrix} (2\pi j f_n)^2 \\ 2\pi j f_n \end{pmatrix} \end{pmatrix} \right) \delta$$

where

$$\beta_i = (\kappa - \hat{\kappa}) \begin{bmatrix} 0 & (2\pi j f_n)^2 \\ 0 & 0 \end{bmatrix}$$

Through further calculation, it is found that

$$-2\eta^T\left(\hat{A} - A\right)^T C^T \delta$$
$$= -(\kappa - \hat{\kappa})(2\pi f_n)^3 \left(\eta_1 + 3^3 \eta_3 + \cdots + (2n-1)^3 \eta_{2n-1}\right)$$

If the following parameter update law is selected

$$\dot{\hat{\delta}} = (2\pi f_n)^3 \left(1^3 \eta_1 + 3^3 \eta_3 + \cdots + (2n-1)^3 \eta_{2i-1}\right) \delta \qquad (10)$$

Then eq. (9) becomes,

$$\dot{V}\left(\delta, \kappa - \hat{\kappa}\right) \leq 0$$

This shows the global stability (*i.e.* boundedness) of the LSM observer. By the La Salle's invariance principle $\dot{V}(\delta, \kappa - \hat{\kappa}) = 0$ implies that $\delta = 0$. Then it is possible to show the asymptotic stability of the closed-loop system. In recent adaptive estimation literature [28], it has been found that nonlinear injection of the output estimation error can reduce the convergence time. Following the ideas presented in [28], the parameter identification law (10) can be modified as:

$$\dot{\hat{\delta}} = (2\pi f_n)^3 \left(1^3 \eta_1 + 3^3 \eta_3 + \cdots + (2n-1)^3 \eta_{2i-1}\right) \lfloor \delta \rceil^\alpha \qquad (11)$$

where $\lfloor \delta \rceil^\alpha = |\delta|^\alpha \mathrm{sgn}\left(\delta\right), \alpha \in [0,1)$. Although (11) reduces the convergence time but the closed-loop system is no longer globally stable. Only local stability can be achieved around the equilibrium point $\delta = 0$. However this is sufficient from the practical point of view. As such for further development, identification law (11) will be used. Using $\hat{\kappa}$ and η, the state variables of the original system (given in eq.(3)) can be estimated as:

$$\hat{x} = T^{-1}\eta \qquad (12)$$

where

$$T^{-1} = \begin{bmatrix} T_1^{-1} & 0 & \cdots & 0 \\ 0 & \ddots & 0 & \vdots \\ \vdots & & \ddots & 0 \\ 0 & \cdots & 0 & T_n^{-1} \end{bmatrix} \Bigg($$

with

$$T_i^{-1} = \begin{bmatrix} ((2i-1)2\pi f_n)^2 & (2i-1)2\pi f_n \\ -\hat{\kappa}((2i-1)2\pi f_n)^3 & ((2i-1)2\pi f_n)^2 \end{bmatrix} \Bigg($$

With the values of $\hat{\kappa}$ and $\hat{x}$, the parameters of the harmonics polluted grid voltage signal can be estimated as:

$$\hat{f}_i = \sqrt{\hat{\kappa}}(2i-1)f_n, \qquad (13a)$$

$$\hat{\theta}_i = \arctan \frac{\hat{x}_{2i-1}2\pi \hat{f}_i}{\hat{x}_{2i}} \Bigg) \Bigg(\qquad (13b)$$

To implement the proposed LSM observer, eq. (6), (11), (12) and (13) are required. Block diagram representation is given in Fig. 1.

Fig. 1 Block diagram of the proposed LSM observer based single-phase grid voltage parameter estimation technique.

2.2 Gain tuning

In this Section, the tuning of the gain matrix L and K along with the constant α in eq. (11) are going to be detailed. To tune the Luenberger gain matrix L, first the desired closed loop poles need to be selected. For the sake of simplicity, let us consider the case where the grid voltage signal contains the fundamental frequency along with third order harmonics. In this case, the eigenvalues of the system matrix, A (given in eq.(5)) are $\pm i\omega_n$ and $\pm i3\omega_n$. Then the desired closed-loop poles can be chosen as two times the fundamental frequency of the individual components i.e. $-2 \times \omega_n$, $-2 \times \omega_n$, $-2 \times 3\omega_n$, and $-2 \times 3\omega_n$. From theoretical point of view, the closed-loop poles can be chosen higher than two times the fundamental frequency. However, this may introduce numerical instability as the observer gains would be too high. Moreover, very fast closed-loop poles will deteriorate the transient performance in terms of very high peak overshoot. As such the selected poles can be considered as a trade-off between between fast dynamic response and acceptable peak overshoot.

With the selected closed-loop poles choice, by using Matlab command acker, the observer gain matrix L can be easily found. For the case of higher order harmonics, one suggested choice of closed loop poles are 2 times the angular frequency value. For choosing the sliding mode gain matrix K part of the observer, we can start with the gain L. A suitable choice for K can be $K = \rho L, \rho > 0$. The value of ρ should be chosen as a very small constant. In the LSM observer, the main job is done by the Luenberger part while the sliding mode part is there to provide the robustness. Finally, $\mu \in [0, 1)$ in eq. (11) determines the speed of the frequency adaptation. Lower value of α decreases the convergence time, however, effects the transient performance specially maximum peak overshoot. If higher values of μ is selected, it increases the convergence time but at the same time reduces the maximum peak overshoot significantly. As such the choice of α is up to the designer. $\alpha = 0.5$ can be selected as the starting point.

3 Experimental Results

This section details the experimental validation of the proposed LSM observer technique. We have used dSPACE ®1104 board as the rapid prototyping tool. In this

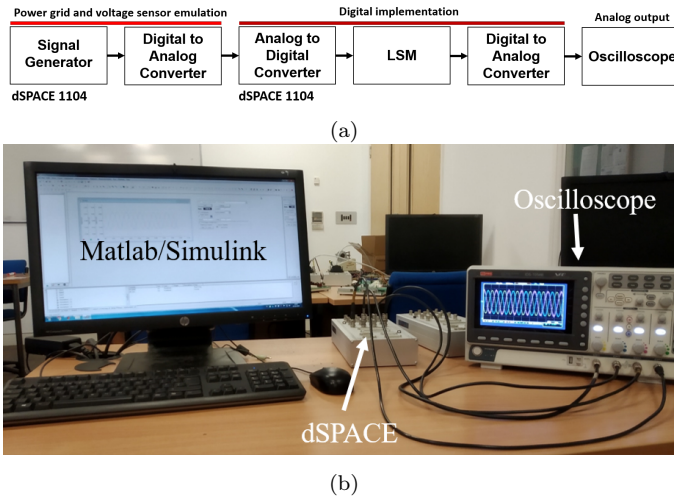| Proposed Luenberger Sliding Mode Observer |
|---|
| Desired closed loop poles: $-2\omega_n$, $-6\omega_n$, $-10\omega_n$ |
| Observer Gain, $L = [0.1136; 53.87; -0.0151; 35.22; -0.006; -11.69]$ |
| Frequency update law parameters: $\mu = 0.5$ and $\rho = 10^{-4}$ |
| Multi-resonant second order generalized integrator- frequency locked-loop (MSOGI-FLL) |
| SOGI gain, $k = \sqrt{2}$, FLL gain, $\varGamma = 50$. |

Table 1 Control Parameters For Comparative Experimental Study.

(a)

(b)

Fig. 2 Experimental setup, (a): overview, (b): actual setup.

approach, dSPACE was used to generate the grid voltage signal which was then converted from digital to analog through digital-to-analog converter (DAC). This can be considered as an emulation of the grid voltage signal. This analog signal was then converted through an analog-to-digital converter (ADC) to be fed into the digital implementation of the proposed LSM observer. This type of experimental study is quite common in the literature e.g. [31, Fig. 12]. The overview of the experimental setup and the actual experimental setup is given in Fig. 2.

The proposed LSM observer was implemented in Simulink and discretized using the Runge-Kutta solver with a sampling frequency was 10 KHz. As a comparison tool, we have selected the multi-resonant second order generalized integrator- frequency locked-loop (MSOGI-FLL) given in Fig. 8 of [29]. Single frequency SOGI-FLL has excellent dynamic performance. However, there is always some steady-state error in the presence of harmonics. MSOGI-FLL uses multiple SOGI block tuned different frequencies to get rid of the steady-state error completely. As such MSOGI-FLL can be considered as an effective tool for parameter estimation in the presence of harmonics. The MSOGI-FLL is discretized using the third-order Adams-Bashforth technique. Control parameters for both techniques are given in Tab. 1. To test the LSM and MSOGI-FLL, we have considered a harmonics polluted grid voltage signal that contains 10% total harmonic distortion (THD) with third and fifth order harmonics. The grid signal is represented by the following equation:

$$y = \sin(120\pi t) + 0.0707\sin(360\pi t) + 0.0707\sin(600\pi t) \tag{14}$$

change→ Settling time↓(in ≈ cycles)	−2Hz. frequency		45° phase		−0.5p.u. amp.	
	LSM	MSOGI-FLL	LSM	MSOGI-FLL	LSM	MSOGI-FLL
±0.1Hz.	1.02	2.75	1.12	3.45	0.85	3.4
±1°	1.08	1.05	1.15	3.25	0.95	3

Table 2 Comparative summary of the presented experimental results.

For signal (14), Both LSM and MSOGI-FLL were of 7-th order. The robustness of the algorithms were tested using the following challenging conditions:

− Test-I: Change of frequency from 60 Hz. to 58 Hz.
− Test-II: Change of phase from $0°$ to $45°$.
− Test-III: Change of amplitude from 1 p.u. to 0.5 p.u.

Results of the experimental studies are given in Fig. 3, 4 and 5 for Test-I, II and III respectively. Comparative summary of the settling times for phase and frequency in different test scenarios can be found in Table 2. These results demonstrate an excellent performance by the LSM technique. Settling times of the LSM technique for frequency and phase estimation are at least 2-3 times faster than the state of the art MSOGI-FLL technique. However, MSOGI-FLL has better peak phase estimation error. This is partly due to the fact that the phase of MSOGI-FLL is obtained by integrating the angular frequency signal. In case of LSM, estimated estates are used. To overcome this problem, one solution would be to use the integration the angular frequency signal for determining the phase. However, this may slow-down the estimation rapidity. As a result, this can be considered as a designer choice. Finally, it can be claimed that the experimental results validated the theoretical developments proposed in Sec. 2.

4 Conclusion

In this work, a frequency adaptive Luenberger Sliding Mode observer has been proposed to estimate the phase and frequency of the single-phase grid voltage signal subject to the presence of harmonics. The observer has been proposed using a parametrized linear dynamical model of the grid voltage signal. The observer depends on the accurate value of the grid frequency parameter. Using Lyapunov stability theory, an adaptation law is proposed for the frequency adaptation. Closed loop stability analysis is also given for the adaptive observer. Experimental validations are provided to show the feasibility of the proposed observer in real-time. A comparative study has been performed with state of the art Multiple SOGI-FLL technique. Experimental results showed that the algorithm provides excellent accuracy and fast convergence even in the presence of non smooth variations in phase, frequency and amplitude. The algorithm is easy to implement and simple tuning rules are also provided. In this work, we have only considered grid synchronization. Considering the dynamics and stability analysis of the complete closed-loop system (inverter+inverter controller+synchronizing observer) would be considered in a future work.
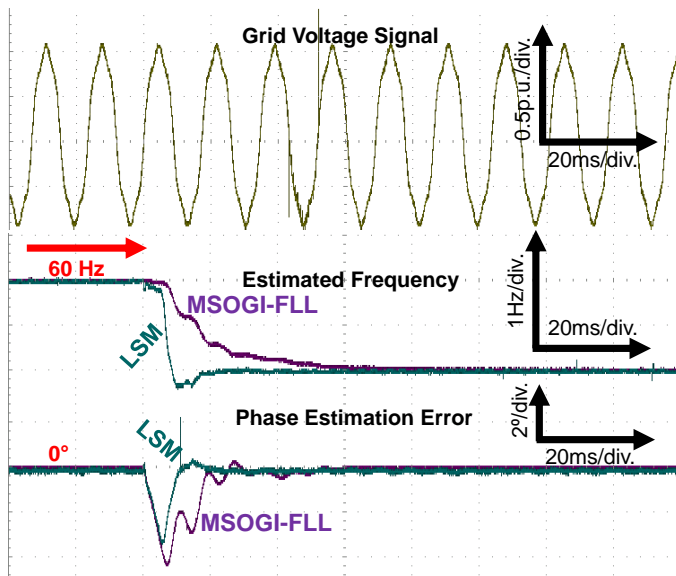
Fig. 3 Comparative experimental results for sudden change of −2 Hz. frequency.
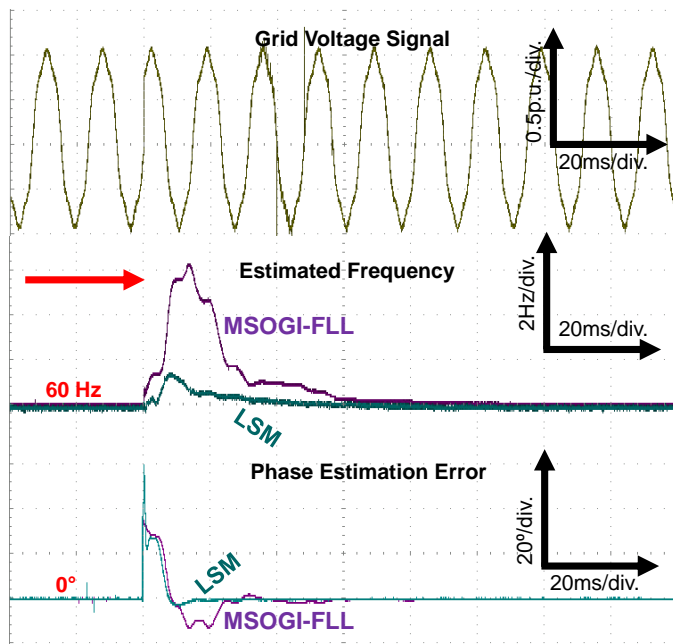

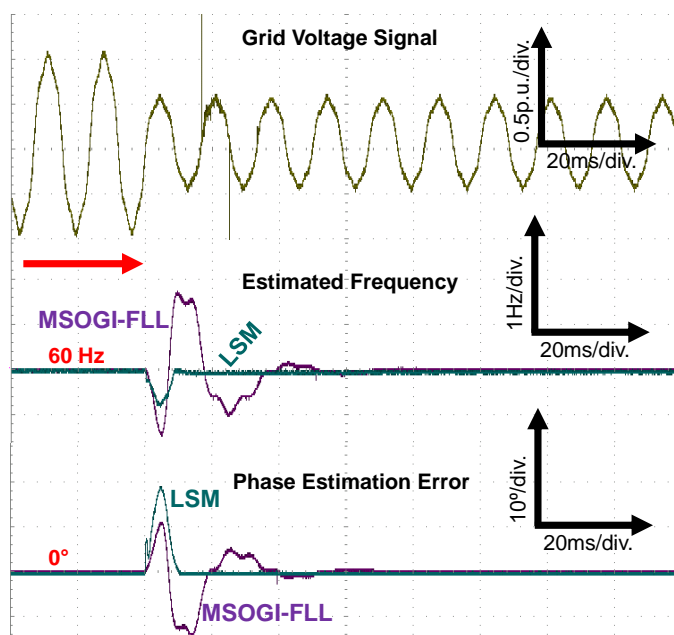**Fig. 4** Comparative experimental results for sudden change of 45° phase.

Fig. 5 Comparative experimental results for sudden change of −0.5 p.u. amplitude.

References

1. Ahmed, H., Amamra, S., Bierhoff, M.: Frequency-locked loop-based estimation of single-phase grid voltage parameters. IEEE Transactions on Industrial Electronics **66**(11), 8856–8859 (2019)
2. Ahmed, H., Amamra, S., Salgado, I.: Fast estimation of phase and frequency for single-phase grid signal. IEEE Transactions on Industrial Electronics **66**(8), 6408–6411 (2019)
3. Ahmed, H., Benbouzid, M.: Simplified second-order generalized integrator-frequency-locked loop. Advances in Electrical and Electronic Engineering **17**(4), 405–412 (2019)
4. Ahmed, H., Benbouzid, M.: Demodulation type single-phase PLL with DC offset rejection. Electronics Letters (2020). DOI 10.1049/el.2019.3718
5. Ahmed, H., Benbouzid, M., Ahsan, M., Albarbar, A., Shahjalal, M.: Frequency adaptive parameter estimation of unbalanced and distorted power grid. IEEE Access **8**, 8512–8519 (2020)
6. Ahmed, H., Bierhoff, M., Benbouzid, M.: Multiple nonlinear harmonic oscillator-based frequency estimation for distorted grid voltage. IEEE Transactions on Instrumentation and Measurement pp. 1–9 (2019). DOI 10.1109/TIM.2019.2931065
7. Ahmed, H., Pay, M.L., Benbouzid, M., Amirat, Y., Elbouchikhi, E.: Hybrid estimator-based harmonic robust grid synchronization technique. Electric Power Systems Research **177**, 106,013 (2019)
8. Ahmed, H., Pay, M.L., Benbouzid, M., Amirat, Y., Elbouchikhi, E.: Gain normalized adaptive observer for three-phase system. International Journal of Electrical Power & Energy Systems **118**, 105,821 (2020)
9. Bierhoff, M.H.: A general PLL-type algorithm for speed sensorless control of electrical drives. IEEE Transactions on Industrial Electronics **64**(12), 9253–9260 (2017)
10. Biricik, S., Khadem, S.K., Redif, S., Basu, M.: Voltage distortion mitigation in a distributed generation-integrated weak utility network via a self-tuning filter-based dynamic voltage restorer. Electrical Engineering **100**(3), 1857–1867 (2018)
11. Biricik, S., Komurcugil, H.: Optimized sliding mode control to maximize existence region for single-phase dynamic voltage restorers. IEEE Transactions on Industrial Informatics **12**(4), 1486–1497 (2016)

12. Biricik, S., Redif, S., Khadem, S.K., Basu, M.: Improved harmonic suppression efficiency of single-phase apfs in distorted distribution systems. International Journal of Electronics **103**(2), 232–246 (2016)
13. Büyük, M., Tan, A., Tümay, M.: Improved adaptive notch filter-based active damping method for shunt active power filter with LCL-filter. Electrical Engineering **100**(3), 2037–2049 (2018)
14. Choqueuse, V., Belouchrani, A., Auger, F., Benbouzid, M.: Frequency and phasor estimations in three-phase systems: Maximum likelihood algorithms and theoretical performance. IEEE Transactions on Smart Grid **10**(3), 3248–3258 (2019)
15. Filippov, A.: Differential equations with discontinuous right-hand side. American Mathematical Society Translations **42**(2), 354–362 (1964)
16. Hasan, S.N., Husain, I.: A Luenberger–sliding mode observer for online parameter estimation and adaptation in high-performance induction motor drives. IEEE Transactions on industry applications **45**(2), 772–781 (2009)
17. Khalil, H.K.: Nonlinear control. Prentice Hall, Upper Saddle River, New Jersey (2014)
18. Lievre, A., Pelissier, S., Sari, A., Venet, P., Hijazi, A.: Luenberger observer for SoC determination of lithium-ion cells in mild hybrid vehicles, compared to a Kalman filter. In: Ecological Vehicles and Renewable Energies (EVER), 2015 Tenth International Conference on, pp. 1–7. IEEE (2015)
19. Ma, H., Girgis, A.A.: Identification and tracking of harmonic sources in a power system using a Kalman filter. IEEE Transactions on Power Delivery **11**(3), 1659–1665 (1996)
20. McGrath, B.P., Holmes, D.G., Galloway, J.J.H.: Power converter line synchronization using a discrete Fourier transform (DFT) based on a variable sample rate. IEEE Transactions on Power Electronics **20**(4), 877–884 (2005)
21. Meral, M.E., Çelik, D.: Benchmarking simulation and theory of various PLLs produce orthogonal signals under abnormal electric grid conditions. Electrical Engineering **100**(3), 1805–1817 (2018)
22. Meral, M.E., Çelik, D.: Comparison of SRF/PI-and STRF/PR-based power controllers for grid-tied distributed generation systems. Electrical Engineering **100**(2), 633–643 (2018)
23. Morales-Caporal, M., Rangel-Magdaleno, J., Peregrina-Barreto, H., Morales-Caporal, R.: FPGA-in-the-loop simulation of a grid-connected photovoltaic system by using a predictive control. Electrical Engineering **100**(3), 1327–1337 (2018)
24. Nanda, S., Dash, P., Chakravorti, T., Hasan, S.: A quadratic polynomial signal model and fuzzy adaptive filter for frequency and parameter estimation of nonstationary power signals. Measurement **87**, 274–293 (2016)
25. Oubrahim, Z., Choqueuse, V., Amirat, Y., Benbouzid, M.E.H.: Maximum-likelihood frequency and phasor estimations for electric power grid monitoring. IEEE Transactions on Industrial Informatics **14**(1), 167–177 (2018)
26. Pay, M.L., Ahmed, H.: Modeling and tuning of circular limit cycle oscillator fll with preloop filter. IEEE Transactions on Industrial Electronics **66**(12), 9632–9635 (2019)
27. Qasim, M., Kanjiya, P., Khadkikar, V.: Artificial-neural-network-based phase-locking scheme for active power filters. IEEE Transactions on Industrial Electronics **61**(8), 3857–3866 (2014)
28. Ríos, H., Efimov, D., Perruquetti, W.: An adaptive sliding-mode observer for a class of uncertain nonlinear systems. International Journal of Adaptive Control and Signal Processing **32**(3), 511–527 (2018)
29. Rodríguez, P., Luna, A., Candela, I., Mujal, R., Teodorescu, R., Blaabjerg, F.: Multiresonant frequency-locked loop for grid synchronization of power converters under distorted grid conditions. IEEE Transactions on Industrial Electronics **58**(1), 127–138 (2011)
30. Ruppert, M.G., Karvinen, K.S., Wiggins, S.L., Moheimani, S.R.: A Kalman filter for amplitude estimation in high-speed dynamic mode atomic force microscopy. IEEE Transactions on Control Systems Technology **24**(1), 276–284 (2016)
31. Safa, A., Berkouk, E.M., Messlem, Y., Chedjara, Z., Gouichiche, A.: A pseudo open loop synchronization technique for heavily distorted grid voltage. Electric Power Systems Research **158**, 136–146 (2018)
32. Salgado, I., Chairez, I., Moreno, J., Fridman, L.: Design of mixed Luenberger and sliding continuous mode observer using sampled output information. In: Decision and Control (CDC), 2010 49th IEEE Conference on, pp. 5138–5143. IEEE (2010)
33. Stojić, D., Georgijević, N., Rivera, M., Milić, S.: Novel orthogonal signal generator for single phase PLL applications. IET Power Electronics **11**(3), 427–433 (2018)

34. Teodorescu, R., Blaabjerg, F., Liserre, M., Loh, P.C.: Proportional-resonant controllers and filters for grid-connected voltage-source converters. IEE Proceedings-Electric Power Applications **153**(5), 750–762 (2006)
35. Vidal, A., Freijedo, F.D., Yepes, A.G., Fernandez-Comesaña, P., Malvar, J., Lopez, O., Doval-Gandoy, J.: A fast, accurate and robust algorithm to detect fundamental and harmonic sequences. In: Energy Conversion Congress and Exposition (ECCE), 2010 IEEE, pp. 1047–1052. IEEE (2010)
36. Yang, Y., Hadjidemetriou, L., Blaabjerg, F., Kyriakides, E.: Benchmarking of phase locked loop based synchronization techniques for grid-connected inverter systems. Proc. ICPE ECCE Asia pp. 2517–2524 (2015)